INTERNATIONAL JOURNAL OF PRECISION ENGINEERING AND MANUFACTURING Vol. 14, No. 6, pp. 1071-1078 JUNE 2013 / 1071
DOI: 10.1007/s12541-013-0144-5

Heuristic Optimization Method for Cellular Structure Design of Light Weight Components

Jason Nguyen[1], **Sang-in Park**[1], and **David Rosen**[1,#]

1 The George W. Woodruff School of Mechanical Engineering, Georgia Institute of Technology, Atlanta, GA, USA
Corresponding Author / E-mail: david.rosen@me.gatech.edu, TEL: +1-404-894-9668, FAX: +1-404-894-9342

KEYWORDS: Heuristic optimization method, CAD, Additive manufacturing, Cellular structure, Meso-scale lattice structure, Design

Additive manufacturing can be used to produce structures which would be impossible to manufacture using traditional manufacturing processes. One application of this technology is for fabrication of customized, light-weight material called meso-scale lattice structure (MSLS), which is a type of cellular structure with dimensions in the range of 0.1 to 10 mm. The problem to be addressed in this paper is how to efficiently synthesize MSLS with thousands of struts and, hence, thousands of design variables. A heuristic optimization method is presented for efficiently synthesizing large MSLS on complex shaped parts that reduces the multivariate optimization problem to a problem of only two variables. The heuristic is based on the observation that the stress distribution in a MSLS will be similar to the stress distribution in a solid body of the same overall shape. Based on local stress states, unit cells from a predefined unit-cell library are selected and sized to support those stress states. In this paper, the method is applied to design a strong, stiff, and light-weight Micro Air Vehicle fuselage. Weight savings are demonstrated as a result.

Manuscript received: September 11, 2012 / Accepted: April 26, 2013

NOMENCLATURE

MSLS = Meso-Scale Lattice Structures
SMS = Size Matching and Scaling Method
CLS = Conformal Lattice Structures

1. Introduction

Additive manufacturing (AM) refers to the use of layer-based additive processes to manufacture finished parts by stacking layers of thin 2-D cross-sectional slices of materials. This process enable fabrication of parts with high geometric complexity, material grading, and customizability.[1]

Design for manufacturing (DFM) has typically meant that designers should tailor their designs to eliminate manufacturing difficulties and minimize costs. However, AM capabilities now provide an opportunity to re-think DFM to take advantage of the uniqueness of these technologies.[2] Several companies are now using AM technologies for production manufacturing. For example, Siemens, Phonak, Widex, and the other hearing aid manufacturers use selective laser sintering (SLS) and stereolithography (SLA) machines to produce hearing aid shells, Align Technology uses SLA to fabricate molds for producing clear braces ("aligners"), and Boeing and its suppliers use SLS to produce ducts and similar parts for F-18 fighter jets. In the first three cases, AM machines enable one-off, custom manufacturing of 10's to 100's of thousands of parts. In the last case, AM technology enables low volume production. In addition, AM can greatly simplify product assembly by allowing parts that are typically manufactured as multiple components to be fabricated as one piece. More generally, the unique capabilities of AM technologies enable new opportunities for customization, improvements in product performance, multi-functionality, and lower overall manufacturing costs. These unique capabilities include: shape complexity, where very complex shapes, lot sizes of one, customized geometries, and shape optimization are enabled; material complexity, where material can be processed one point, or one layer, at a time, enabling the manufacture of parts with complex material compositions and designed property gradients; and hierarchical complexity, where multi-scale structures can be designed and fabricated from the microstructure through geometric mesostructure (sizes in the millimeter range) to the part-scale macrostructure.

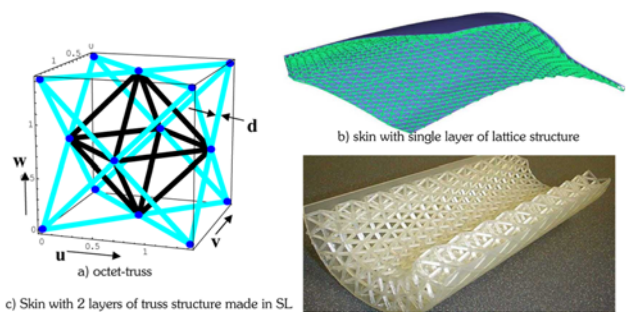

Fig. 1 Octet truss unit cell and example parts with octet truss mesostructure

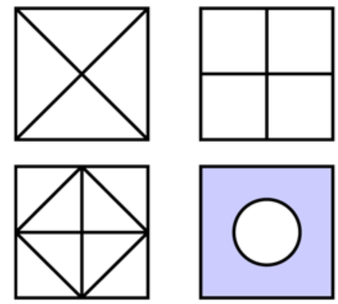

Fig. 2 Cellular primitives: three lattice structures and one web structure

In this paper, we cover two main topics. First, we present geometric construction methods that enable designers to take advantage of the shape complexity capabilities of AM processes. Specifically, we develop a method for constructing cellular materials that conform to the shapes of part surfaces; when restricted to lattice structures we call such constructs Conformal Lattice Structures™ (CLS). The software that embodies this process is integrated into a commercial computer-aided design (CAD) system. Second, we present a design method, the augmented size matching and scaling (SMS) method, to optimize CLS efficiently and systematically.

1.2 Cellular Materials

The concept of designed cellular materials is motivated by the desire to put material only where it is needed for a specific application. From a mechanical engineering viewpoint, a key advantage offered by cellular materials is high strength accompanied by a relatively low mass. These materials can provide good energy absorption characteristics and good thermal and acoustic insulation properties as well.[3] Cellular materials include foams, honeycombs, lattices, and similar constructions. When the characteristic lengths of the cells are in the range of 0.1 to 10 mm, we refer to these materials as mesostructured materials. Mesostructured materials that are not produced using stochastic processes (e.g. foaming) are called designed cellular materials. In this paper, we focus on designed lattice materials called meso-scale lattice structure (MSLS).

The area of lattice materials has received considerable research attention due to their inherent advantages over foams in providing light, stiff, and strong materials. Lattice structures tend to have geometry variations in three dimensions; some of our designs are shown in Figure 1. Lattices can be three times stronger than foams due to the nature of material deformation: the foam is governed by cell wall bending, while lattice elements stretch and compress.[4]

In order to effectively design cellular structures, we must be able to accurately model, determine the mechanical properties, and quantify the performance of these structures. Many methods have been developed to analyze various cellular structures, including for metal foams,[3] honeycombs,[5] and lattice structures with simplified models[4] and more complex 3D frame analysis.[6]

1.3 Design Methods

The design synthesis method for cellular materials consists of size, shape, and topology optimization to address different aspects of the structural design problem. In order to understand optimization of structures, the definitions of three categories of structural optimization are important.[7] A typical size optimization involves finding the optimal cross-sectional area of each strut in a truss structure. Shape optimization computes the optimal form that defined by the boundary curves or boundary surfaces of the body.[8] The process may involve moving nodes to change the shape of the structure; however, the element-node connectivity remains intact. Topology optimization, according to Rozvany, finds optimal connective or spatial sequences of members or elements in a structure.[9] In topological optimization, the physical size, shape, and connectivity of the structure are not known. The only known properties are the volume of the structure, the loads, and the boundary conditions.[7] It can be seen that topology optimization involves aspects of both size and shape optimization. Size and shape optimizations consider the material distribution in the structure to satisfy certain loading conditions while maintaining the same topology. On the other hand, the initial and optimal structures are completely different in the case of topology optimization. In this research, optimization variables of the truss structures are strut diameters. However, each unit cell of the MSLS can have a different configuration depending on the selection criteria. Therefore, "topology optimization' will be the term used in this research for designing and optimizing MSLS.

The topology optimization techniques used to design truss structures are based on one of two approaches: the homogenization (continuum) approach and the ground (discrete) truss approach. Analytical solutions are possible under limited conditions and are known as Michell trusses.[10] The homogenization approach is a material distribution method that considers the design space as an artificial composite material with a large number of periodically distributed small holes. The sizes of these small holes are the design variables. In the final optimal structure, regions with small holes are filled while regions with large holes are considered empty.[11]

The ground truss approach starts with a ground structure, which is a grid of all elements connecting the nodes in the design space. The optimal truss structure is realized by selecting an optimal substructure from this pre-defined ground structure. Ultimately, the ground-truss approach is a sizing optimization problem, where the cross-sections of ground truss members are the continuous design variables for the optimization. The cross-sections of the struts are sized to support the applied loads on the structure. Struts with cross-sections near zero are then removed to obtain the optimal structure.

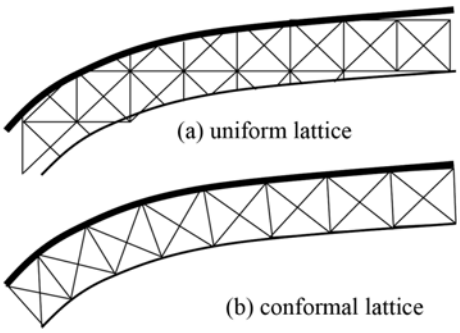

Fig. 3 Uniform and conformal lattice structures

2. CLS Design Method

The basic idea of how cellular materials are created is presented here. Four example primitive cell types are shown in Figure 2, three of which are lattice structures and the fourth is a foam. These cell types are 2-dimensional for simplicity of presentation. The octet lattice in 1a is an example 3-D cell type. Lattice structures consist of a set of struts (beams) that connect the nodes of the lattice.

To generate the cellular designs in Figure 1, the primitive cell types must be mapped into a mesh. In 2-D, the mesh consists of a set of connected quadrilaterals. In 3-D the mesh consists of hexahedra (6-sided volume elements). The uniqueness of our work is our use of conformal cellular structures, rather than uniform “lattice block” materials, that can be used to stiffen or strengthen a complex, curved surface. To observe the difference, Figure 3(a) is an example uniform lattice structure, while Figure 3(b) shows a conformal lattice. Meshes for uniform structures consist of cube elements in 3-D (squares in 2-D), while for conformal structures, the mesh elements are general hexahedra. We have developed a new algorithm for generating conformal meshes that are used to create conformal lattice and cellular structures, based on an older free meshing algorithm.[12]

The overall algorithm for generating conformal cellular structures consists of two main stages: computing 3D conformal mesh, and populating the mesh with cells. The objective of the meshing algorithm is to generate a conformal hexahedral mesh into which cells from the cell library can be placed. One or more layers of cellular structure can be placed to support the part’s skin. The input to the algorithm may be a CAD solid model of the part, a surface model of the part, or a triangulated surface model (STL file) of the part.[12]

The algorithm to generate a 3-D conformal mesh consists of six main steps. The first step is to divide the part boundary into relatively flat regions, since it is easier to control the mesh generation method if regions are not very curved.

For each region, three operations are performed, corresponding to Steps 2, 3, and 4. Step 2 computes the offset of the object boundary. We use an offset method developed for tessellated part surfaces,[13] but any offsetting method could be used. Step 3 is to construct a tri-parameter volume between the original surface and its offset. This step of the algorithm imposes a surface parameterization on the region of the part that will be reinforced.[14] The same parameterization is transferred to the offset surface. Finally, a lofted volume is constructed from the original surface to the offset surface. The fourth step is to generate the conformal mesh by dividing the parameterized volume into individual elements (hexahedra). The final step is to ensure that region boundaries match by adjusting node positions and by adding elements, if necessary.

The algorithm for the second stage (populate mesh with cells) of the overall CLS design method is described here. One input to the algorithm is the conformal hexahedral mesh that was generated in the first step. The other input is the cell types contained within a library. The first step is to partition the mesh elements into regions such that within each region the loading conditions are similar on each element. These need not be the same regions that were used for mesh construction. For each region, a cell type from the cell type library is selected to populate the mesh elements in that region. The idea is to match the region’s loading conditions to the cell type, such that the cell type is effective at supporting the loading conditions. In this manner, the resulting cellular structure is more likely to be lighter for a given level of stress or deflection. These operations may be performed concurrently or maybe performed sequentially, depending upon the designer’s preference and may be automated or be performed by the designer directly.

To construct a STL of the CLS, additional geometric construction operations must be performed. We utilize the approach described in,[12] where solid models of the half-struts incident at each node of the mesh are constructed using Boolean operations in a solid modeling system. Then, each solid “node” is tessellated and the triangles are written to a STL file.

As a final note, the algorithms presented here have been embodied into a C++ software system, one version of which has been integrated into the Siemens NX CAD system.

3. Augmented Size Matching and Scaling (SMS) Method

Regardless of which structural optimization approach is used for the design of meso-scale lattice structures (MSLS), an actual multi-variable optimization routine must be performed. Since the computational complexity of the design problem often scales exponentially with the number of design variables, topology optimization is infeasible or impractical for large design problems. The Size Matching and Scaling (SMS) method uses a heuristic to reduce the multivariable optimization problem to a problem of only two variables.[15] The heuristic is based on the observation that the stress distribution in a MSLS will be similar to the stress distribution in a solid body of the same overall shape. Based on the computed local stress states from the solid body analysis, unit cells from a predefined unit-cell library are selected and sized to support those stress states. The optimal diameters of these struts are then computed by performing a two-variable optimization. This design approach removes the need for a rigorous multi-variable topology optimization, which is a main bottleneck in designing MSLS. A new augmented SMS method presented here integrates the CLS construction methods outlined in Section 2 to the ground structure generation process of the SMS method.

3.1 Problem Formulation

SMS design problems will be formulated using the Compromise Decision Support Problem (cDSP),[16] which is a multi-objective

Table 1 Mathematical cDSP formulation of the SMS problem[15]

Given:	$p^{BG}, p^{F}, p^{M}, p^{UC}, S^{L}_{i,j}, i, k$	
Find:	$D_{i,k} = S^{u}_{i,j} \times S^{L}_{i,j} \times (D_{MAX} - D_{MIN}) + D_{MIN}$	(a)
	D_{MAX}, D_{MIN}	(b)
	$S^{u}_{i,j} = \dfrac{\sum \sigma_n - \sigma^{min}_{i,j}}{\sigma^{max}_{i,j} - \sigma^{min}_{i,j}}$	(c)
Satisfy:	$D_{LB} \le D_{MIN} \le D_{MAX} \le D_{UB}$	(d)
	$\sigma_i \le \sigma_{max}$	(e)
	$V \le V_{max}$	(f)
Minimize:	$Z = (W_d \times d)^2 + \left(W_V \times \dfrac{V - V_t}{V_t}\right)^2$	(g)

formulation based on goal programming, as presented in Table 1.

The symbols p^{BG}, p^{F}, p^{M} represent the boundary, loading and material properties, respectively. The strut diameter, D_i, can either range from the lower diameter bound, D_{LB}, to the upper diameter bound, D_{UB}, or zero. The symbol σ_i represents the axial stress value in each i strut. The symbols V and d represent the volume and the deformation of the structure. W_d and W_V represent weighting variables for d and V in the minimization function, Z. The volume of the structure is calculated by summing the volume of all the struts in the structure, which are assumed to be cylinders:

$$V = \sum \pi \times \frac{D_i^2}{4} \times l_i \tag{1}$$

where l_i represents the length of the i strut. The symbols i, j, and k represent each unit-cell region in the structure, each unit-cell configuration in the unit-cell library, and the strut number in each of the j configurations in the library, respectively; n represents the nodes from the solid-body finite element analysis.

The SMS method requires additional information besides the starting topology, and the boundary condition. External sources of information include the unit-cell library and the solid-body finite element analysis. Using that information, the determination of the strut diameters, shown in (a) of Table 1, reduces to a 2-variable optimization problem. It can be seen that $D_{i,k}$ can be determined using the pre-scaled maximum and minimum diameter value, D_{MAX} and D_{MIN}, a stress scaling factor from the unit-cell library, $S^{u}_{i,j}$, and a unit-cell scaling factor from the solid-body stress analysis, $S^{L}_{i,j}$. Hence, only D_{MAX} and D_{MIN} need to be determined through optimization. The objective function, (g) of Table 1, is formulated in the least-squares format to minimize the deflection of the structure, d, and deviation of the structural volume from a target volume, V_t. W_d and W_V represent the weighting variables for d and V.

The optimization process of D_{MAX} and D_{MIN} requires calculation of deflection, volume, and associate stresses using finite element analysis of the truss structure. The finite-element package, which assumes each truss member as a beam element, was developed in MATLAB.[14] Once the optimization is done, the diameter of each strut is obtained using

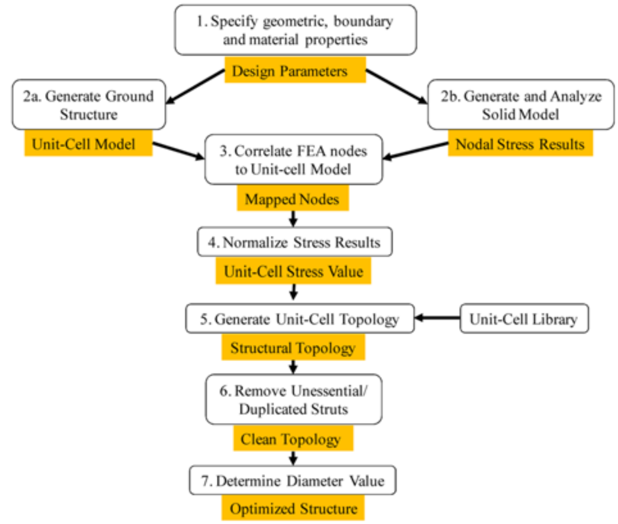

Fig. 4 Overview of augmented SMS method

Equation (a). The optimized maximum and minimum diameters of the structure are denoted as D_{max} and D_{min} to differentiate from the pre-scaled maximum and minimum diameter value, D_{MAX} and D_{MIN}. It is important to note that the finite element analysis of the truss structure is conducted using the scaled/true diameters of the structure. Other problem formulations with different objective functions can also be used with the SMS method.

3.2 Overview of Augmented SMS method

The SMS method can be divided into eight discrete tasks that are completed in seven steps, as summarized in Figure 4. Outputs of each step are shown in the shaded box under each step.

Step 1: Specification of loading, boundary conditions and material properties: Boundary conditions, material properties, and loading conditions are specified for the target meso-scale lattice structure. These properties will be utilized to perform the stress analysis of both the solid-body representation in step 2b and the truss structure during the optimization process of step 7.

Step 2a: Generation of ground structure: In this step of the method, the hexahedral mesh of the MSLS is created using the algorithm described in Sec. 2. The user decides the size of the unit cells.

Step 2b: Solid body finite-element analysis: A solid body is generated that envelopes the part model surfaces and the MSLS and a stress analysis is performed using finite-element analysis using the loading and boundary conditions, and material properties as specified in step 1 of the method. After the analysis is complete, the von Mises stress distribution of the structure provides the general state of stress at each node, which is characterized by six independent normal and shear stress components, σ_{xx}, σ_{yy}, σ_{zz}, σ_{xy}, σ_{xz}, and σ_{yz}.

Step 3: Map FEA nodes to ground structure: In order to use the finite-element analysis result obtained from step 2b, the stress results must be appropriately mapped to the ground structure. The goal of this step is to determine which finite-element nodes correlate to which unit-cell region in the ground structure.

A point containment problem is solved for each node in order to find which unit-cell region it is in. If the node is inside of each of the 6 faces of a unit-cell, then it is contained in that cell. If it lies on the

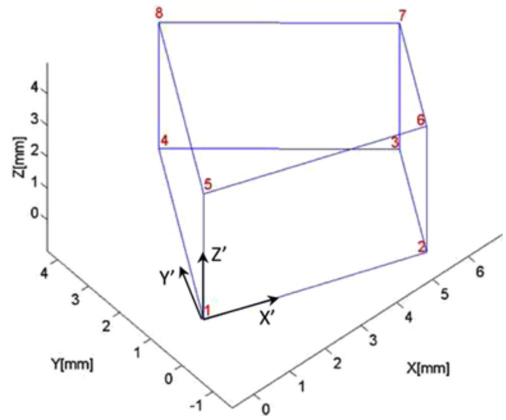

Fig. 5 Unit-cell region

boundary of two cells, then it is included in both. After the node mapping process is done, each unit cell will contain a list of finite element nodes that will be included in the calculation of the stress distribution in that unit cell.

Step 4: Stress Scaling and Normalization: After step 3 is complete, the stress values from the finite-element nodes in each unit cell are averaged to determine average stress values of the six independent normal and shear stress components. The stress distribution is of interest and will be used to guide the setting of strut sizes. Therefore, the stresses are normalized from zero to one such that the largest value of stress is equal to one. These six scaling values correlate to six entries of each configuration in the unit cell.

In topology generation, the diameter values of the selected unit-cell configuration from the preconfigured unit-cell library are scaled against the associated stress values (σ_{xx}, σ_{yy}, σ_{zz}, τ_{xy}, τ_{xz}, and τ_{yz}) and then mapped to the unit cells in the ground structure. However, since the solid-body results are provided relative to the global coordinate system, stress transformations are needed to ensure correct topology generation, which is performed by rigid-body rotation of the axes. Since the unit cell is not necessarily a cuboid hexahedron, a representative local coordinate system must be determined. Each unit cell, such as in Figure 5, is characterized by 8 nodes and 12 edges. Three edges of the unit cell, edge 1-2, edge 1-4, and edge 1-5, respectively, are selected as reference edges, nominally representing the x, y, and z axes, respectively. An orthogonal local coordinate system, indicated by X'-Y'-Z', is constructed centered at node 1 using the reference edges as guides. Details are in.[17]

After obtaining the local coordinate system for the unit cell, the relative orientation between the local (X'Y'Z') and global coordinate (XYZ) system can be determined. Using a standard approach with rotation matrices and direction cosines, the transformation from the XYZ to the X'Y'Z', system is given as

$$\begin{Bmatrix} x' \\ y' \\ z' \end{Bmatrix} = \begin{bmatrix} \cos(\alpha_1) & \cos(\beta_1) & \cos(\theta_1) \\ \cos(\alpha_2) & \cos(\beta_2) & \cos(\theta_2) \\ \cos(\alpha_3) & \cos(\beta_3) & \cos(\theta_3) \end{bmatrix} \begin{Bmatrix} x \\ y \\ z \end{Bmatrix} \quad (2)$$

where $\cos(\alpha_1)$, $\cos(\beta_1)$, $\cos(\theta_1)$ are the direction cosines of X' on the global XYZ axes, respectively, and the rotation matrix is denoted R.

The stress state at a point is characterized by six independent normal and shear stress components, which can be organized into a matrix:

$$\begin{bmatrix} \sigma_{xx} & \tau_{xy} & \tau_{xz} \\ \tau_{yx} & \sigma_{yy} & \tau_{yz} \\ \tau_{zx} & \tau_{zy} & \sigma_{zz} \end{bmatrix} \quad (3)$$

The grouping of these stress components becomes the components of a second-order stress tensor, which is defined in the deformed state of the material and is known as the Cauchy stress tensor.[18] The Cauchy stress tensor in the local coordinate system can be obtained using Eqn. 4.

$$[\sigma'] = R[\sigma]R^T \quad (4)$$

R^T is the transpose of R, and s and σ' are the Cauchy stress tensors in global and local coordinate systems, respectively.[18] Ultimately, there will be six stress values for each unit cell, σ_{xx}, σ_{yy} σ_{zz}, τ_{xy}, τ_{xz}, τ_{yz}, which correspond to the scaling factors, $S^u_{i,j}$, in (a) of Table 1.

Step 5: Topology generation: The unit-cell lattice structure selection and mapping process will be described in detail in Section 3.3. After this step is complete, the structure will have a topology designed for the anticipated stress distribution in the truss structure. The relative thickness of one strut to another is known based on step 4. However, these normalized diameters must be correlated with actual strut diameter values in step 7 of the method.

Step 6: Ambiguity resolution: Since the unit cells are populated individually, there will be instances of overlapping struts between adjacent unit cells. To resolve this ambiguity, the largest diameter strut is kept and all other smaller struts are removed. Duplicated nodes are also removed.

Step 7: Diameter Sizing: The normalized strut diameters must be replaced with the actual diameter values to satisfy the loading and volume condition. It can be seen from the problem formulation, Table 1, the only parameters missing to determine the diameter of each strut are D_{MIN} and D_{MAX}, the pre-scaled thinnest and thickest diameters, respectively. After D_{MIN} and D_{MAX} are calculated, the diameters of each strut can be determined using Eqn. 5.

$$D_{i,k} = S^u_{i,j} \times S^L_{i,j} \times (D_{MAX} - D_{MIN}) + D_{MIN} \quad (5)$$

In the 2-variable approach, values D_{MIN} and D_{MAX} are determined by performing 2-variable minimization of the objective function (g) in Table 1. It is rewritten in Eqn. 6 as a function of both D_{MIN} and D_{MAX}, where V (D_{MIN}, D_{MAX}), volume, and d (D_{MIN}, D_{MAX}), deformation, are functions of only D_{MIN} and D_{MAX}. Deformation, d, represents any unit of measure that is directly proportional to structural stiffness, such as tip deflection or strain energy. The target structure must attempt to minimize both volume and deflection, which are competing objectives. The target deflection is usually set to zero. Two algorithms used to perform this two-variable minimization are the Levenburg-Marquardt and active-set algorithms. The Levenburg-Marquardt algorithm has documented success in design and optimization of MSLS,[19] while the active-set algorithm is documented to have success in optimization of multivariable, nonlinear and constrained optimization problems.[20]

$$Z(D_{MIN}, D_{MAX}) = (W_d \times d(D_{MIN}, D_{MAX}))^2 + \left(W_V \times \frac{V(D_{MIN}, D_{MAX}) - V_t}{V_t}\right)^2 \quad (6)$$

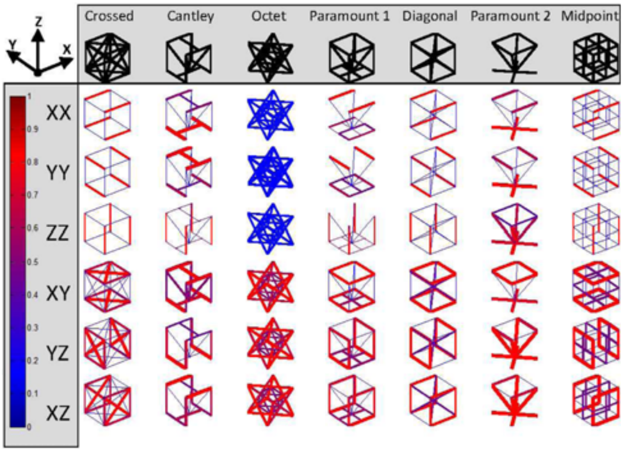

Fig. 6 Unit-cell library[15]

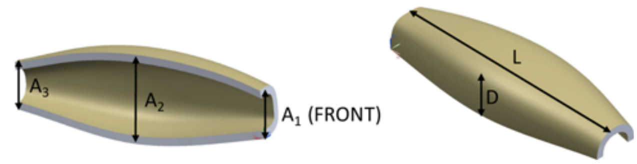

Fig. 7 Multiple views of the fuselage

Table 2 Initial properties for the fuselage

A_1 (mm)	47	L (mm)	254
A_2 (mm)	90	F_{motor} (N)	5.9
A_3 (mm)	45	F_{Tail} (N)	2.7
D (mm)	45	$F_{payload}$ (N/mm^2)	0.1
Unit-cell in-plane (mm)	12	Modulus (N/mm^2)	1960
Unit-cell in-plane (mm)	12	Poisson Ratio	0.3
Unit-cell out-plane (mm)	8	Target Volume (mm^3)	100,000

3.3 Unit-cell Library

The second component of the augmented SMS method is the unit-cell library, which was developed to generate the topology for the MSLS.[15] There are seven different unit-cell configurations in the library. Each configuration has six entries with each specialized for six independent normal and shear stress components. Entries in the library were optimized for loading conditions corresponding to each of the six stress states. The unit-cell library entries are shown in Figure 6. See Ref.[17] for more details.

Unit-cell selection: One way to generate the best topology for the structure is to iteratively populate each unit cell in the ground structure with a configuration from the library and analyze the performance of the structure. However, it is computationally infeasible because there are M^N possible combinations of topologies where M is the number of configurations in the unit-cell library and N is the number of unit cells in the ground structure. Therefore, a heuristic was developed for the selection process.

Since all the configurations of the unit-cell library are optimized such that they have identical performance, the structure with the smallest normalized volume is selected. The selection is performed using the Equation (7),[15] which incorporates three terms. The first is the sum of all lattice structure unit-cell volumes from the 6 stress states. The second term is the volume of the structure if it were mapped into the particular mesh element, while the third term represents a performance term based from empirical results. This term attempts to predict how well a configuration will perform when multiple instances of the configuration are utilized.

This selection process is performed for each unit cell from the ground structure and the configuration with the lowest rating, *r,* is selected and mapped into that unit cell.

$$r = W_v + \sum V_\sigma + W_{vn} + V_{net} + W_p + \sum P \quad (7)$$

where

$$\sum V_\sigma = V_{xx} + V_{yy} + V_{zz} + V_{xy} + V_{xz} + V_{yz} \quad (8)$$

$$\sum P = P_{xx} + P_{yy} + P_{zz} + P_{xy} + P_{xz} + P_{yz} \quad (9)$$

and W_v, W_{vn}, and W_p are weights (importances) on each term.

Unit-Cell Mapping: Once the best possible configuration is determined for a unit cell in the ground structure, it is mapped to that region. If there is a node from the unit-cell configuration that does not exist in the unit cell of the ground structure, it will be added using 3-D linear interpolation. After all the missing nodes are added, the unit-cell configuration can then be populated into the unit cell. The normalized stress values from step 4 of the augmented SMS method are scaled against the normalized diameter values from the unit cell library to determine the relative thickness of one strut to another.

4. Design Example

In order to demonstrate the augmented SMS method, it will be applied to micro aerial vehicle (MAV) fuselage example. Other examples have been explored that serve to validate the augmented SMS method and demonstrate its ability to design large-scale MSLS on complex-shaped parts with curve or non-rectangular surfaces.[17]

MAVs play a critical role in modern military operations as they allow easy surveillance in hazardous environment. The next generation of these aerial robotic systems needs to have enhanced take-off and landing capabilities, better endurance, and be adaptable to mission needs in varying conditions.[21] In terms of the design of the wings and fuselage of these MAVs, some types of structures and/or materials that are lighter, stronger and customizable are highly desired.

In this design example, the fuselage is designed to withstand the impact when landing or crashing. There is a distributed load from the payload applied to the inner surface of the fuselage. The weight of the motor and the tail are modeled as point loads at their centers of mass. This is done in ANSYS using a rigid link element. The equivalent couple is applied to the truss structure. All these weights are scaled by a factor of ten to simulate impact when crashing. The weight of the wing is small and assumed to have negligible contribution. A small area on the bottom of the fuselage is fixed to model the contact zone as the MAV is crashing. Multiple views of the fuselage are shown in Figure 7 with key dimensions labeled. The initial properties of the design problem are provided in Table 2.

Table 3 Optimization results for the fuselage

Optimization Method	Active-Set	Least-squares Min.	Design Space Exploration Scaled
Deflection (mm)	0.299	0.319	0.296
Volume (mm^3)	99973	100010	100000
D_{min} (mm)	0.65	1.12	0.62
D_{max} (mm)	4.16	3.29	4.22
Design Time (s)	1630.9	508.9	76660

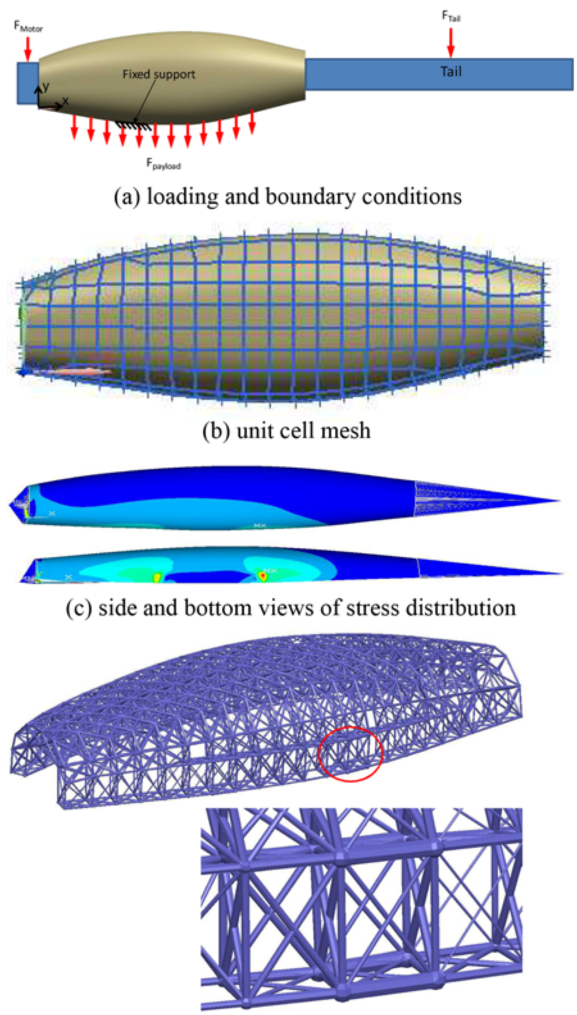

(a) loading and boundary conditions

(b) unit cell mesh

(c) side and bottom views of stress distribution

(d) optimized topology

Fig. 8 Solution process for the fuselage example

The objective is to achieve a target volume of 100,000 mm^3 or 65% porosity relative to the solid model while minimizing deflection. The ground structure for the fuselage is generated by TrussCreator with the desirable unit-cell sizes as provided in Table 2. There are 214 unit cells in the ground structure. The weighting values in Eqn. 7 are set at: $W_v = 0$, $W_{nv} = 1$, $W_p = 5$. With these weighting values, the topology is generated with 101 crossed configurations and 113 diagonal configurations. The topology matches the expectation based on the solid-body analysis. Other topologies were also generated by varying the weighting values. However, this topology has the best structural performance for this particular structure and loading condition. The average displacement of selected nodes on the top of the fuselage, where the large displacement occurs according to the solid-body analysis, is used as the metric for deflection.

The strut diameter results are summarized in Table 3. The active-set method returns the best deflection value but at the expense of design time, taking about three times longer than the Levenburg-Marquardt method. The pre-scaled values of D_{MIN} and D_{MAX} for the active set method are 0.5178 mm and 7.1406 mm, respectively. Figure 8 shows the final topology of the MAV design using the active-set method, as well as the results from the intermediate steps.

In addition to the two optimization approaches, design space exploration using grid search was conducted. D_{MIN} and D_{MAX} were iterated from 0.1 mm to 10 mm and with an increment of 0.1 mm to reduce analysis time. Diameter results that return the lowest objective function value are shown in Table 3. The design space exploration diameter values are found to be close to the values obtained from the active-set method. Both two-variable optimizations were able to return results with much less design time than design space exploration. A valley in the design space can be observed near the solution, which might cause the active set method to converge slowly because of the shallow gradient along one direction.

If the starting configuration consisted of diagonal unit-cells with strut diameters of 3 mm, then the MSLS volume would be 150,000 mm^3. After optimization, the structure has 33 percent less volume and a reduced deflection, resulting in significantly reduced fuel consumption over the life of the MAV.

5. Conclusions

In this article, an augmented size matching and scaling design method for the design of conformal lattice structures was presented. This method enables the design and efficient optimization of MSLS on complex-shaped parts by integrating the free-mesh approach in generating conformal lattice structures for the ground structure generation process. In addition, the method removes the need of rigorous large-scale multivariable topology optimization by utilizing a heuristic that reduces the multivariable optimization problem to a problem of only two variables, which combines solid-body analysis and predefined unit-cell library to generate the topology of the structure. Based on this work, the following conclusions can be made:

The core heuristic of the SMS method often succeeds in finding designs that are close to the global optimum, as shown in the paper's example. The heuristic establishes a relative size for each strut in a conformal lattice structure, based on its stress state found by a solid body finite element analysis. A key step is the selection of unit-cell type for each MSLS mesh element. The diagonal and crossed unit cell types are most often selected by the SMS method and can be shown[17] to be the most efficient structural configurations, per volume, of the unit cell types in Figure 6. However, the overall configuration of unit cells in a part is highly dependent on the problem and specific mesh geometry. Least-squares minimization outperformed the active-set method in terms of design time, but was not able to locate the global minimum. In contrast, the active-set method converged close to the minimum found by design space exploration. Due to the trade-off between design time and structural stiffness, the designer must choose which design criteria are more important. Overall, the augmented SMS method can be applied effectively in the design of MSLS with highly optimized stiffness and volume for complex surfaces. This approach removes the need for rigorous topology optimization, which is a main bottleneck in designing MSLS.

ACKNOWLEDGEMENT

The authors gratefully acknowledge support from the US Air Force Research Laboratory, Paramount Industries, Inc. (now part of 3D Systems), and the US National Science Foundation, grant CMMI-1200788. Any opinions, findings, and conclusions or recommendations expressed in this publication are those of the authors and do not necessarily reflect the views of the National Science Foundation.

REFERENCES

1. Rosen, D. W., "Computer-aided design for additive manufacturing of cellular structures," Computer-Aided Design & Applications, App., Vol. 4, No. 5, pp. 585-594, 2007.
2. Gibson, I., Rosen, D. W., and Stucker, B., "Additive Manufacturing Technologies: Rapid Prototyping to Direct Digital Manufacturing," Springer, 2010.
3. Gibson, L. J. and Ashby, M. F., "Cellular Solids: Structure and Properties," Cambridge University Press, 1997.
4. Deshpande, V. S., Fleck, N. A., and Ashby, M. F., "Effective properties of the octet-truss lattice material." J. Mech. Phys. Solids, Vol. 49, No. 8, pp. 1747-1769, 2001.
5. Wang, A. J. and McDowell, D. L., "Yield surfaces of various periodic metal honeycombs at intermediate relative density," Int. J. Plasticity, Vol. 21, No. 2, pp. 285-320, 2005.
6. Johnston, S. R., Reed, M., Wang, H., and Rosen, D. W., "Analysis of Mesostructure Unit Cells Comprised of Octet-truss Structures," Proc. of the The Seventeenth Solid Freeform Fabrication Symposium, 2006.
7. Bendsøe, M. P. and Sigmund, O., "Topology Optimization: Theory, Methods and Applications," Springer, 2003.
8. Allaire, G., "Shape Optimization by the Homogenization Method," Springer, 2002.
9. Rozvany, G. I. N., "Topology Optimization in Structural Mechanics," Springer, 2003.
10. Michell, A. G. M., "Limits of economy material in frame structures," Philosophy Magazine, Vol. 8, pp. 589-597, 1904.
11. Bendsøe, M. P. and Kikuchi, N., "Generating optimal topologies in structural design using a homogenization method," Comput. Methods Appl. Mech. Engrg, Vol. 71, No. 2, pp. 197-224, 1988.
12. Wang, H., Chen, Y., and Rosen, D. W., "A hybrid geometric modeling method for large scale conformal cellular structures," ASME Computers and Information in Engineering Conference, DETC 2005-85366, 2005.
13. Chen, Y., "An accurate sampling-based method for approximating geometry," Computer-Aided Design, Vol. 39, No. 11, pp. 975-986, 2007.
14. Wang, H., "A unit-cell approach for lightweight structure and compliant mechanism," Georgia Institute of Technology, 2005.
15. Chang, P. S. and Rosen, D. W., "The Size Matching and Scaling Method: A Synthesis Method for the Design of Mesoscale Cellular Structures," Int. J. Comp. Int. Manuf., DOI: 10.1080/0951192X.2011.650880.
16. Seepersad, C. C., Allen, J. K., McDowell, D. L., and Mistree, F., "Robust design of cellular materials with topological and dimension imperfections," J. Mech. Des., Vol. 128, No. 6, pp. 1285-1297.
17. Nguyen, J., Park, S. I., and Rosen, D. W., "Heuristic Optimization Method for Cellular Structure Design of Light Weight Components," Proc. of ISGMA, 2012.
18. Malvern, L. E., "Introduction to the Mechanics of a Continuous Medium," Prentice-Hall, 1969.
19. Chu, C., Engelbrecht, S., Graf, G. C., and Rosen, D. W, "A comparison of synthesis methods for cellular structures with application to additive manufacturing," Rapid Proto. J., Vol. 16, No. 4, pp. 275-283, 2010.
20. Portugal, L. F., Judice, J. J., and Vicente, L. N., "A comparison of block pivoting and interior point algorithms for linear least squares problems with nonnegative variables," Math. Comp., Vol. 63, pp. 625-643, 1994.
21. DARPA Public Affairs, "Can You Design, Build, and Fly the Next Generation UAV?" http://science.dodlive.mil (Accessed 4 May 2012)